LA-UR -92-356

CONF-920606 -- 1

LA-UR--92-356

DE92 008437

TITLE AN EXPLOSIVELY DRIVEN FAST SHOCK TUBE

AUTHOR(S) T(AI)-HO TAN, M-6
S(TANLEY) P. MARSH, M-6

SUBMITTED TO 2ND INTERNATIONAL SYMPOSIUM ON INTENSE DYNAMIC LOADING AND ITS EFFECTS; CHENGDU, CHINA; JUNE 9-12, 1992

AN EXPLOSIVELY DRIVEN, FAST SHOCK TUBE*

T. H. Tan and S. Marsh

Los Alamos National Laboratory, Group M-6, MS J970, Los Alamos, NM 87545 USA

A simple, cylindrically configured fast shock tube (FST) has been employed as a tool to investigate the hydrodynamics of plate drive under a very high impulse-loading condition. The shock tube has a high-explosive outer shell and a low-density foam core. The implosion produces a well-defined Mach disk that is then subsequently used to drive a metallic plate. A thin stainless steel (SS) plate has been successfully launched to 9 km/s with this device. The experimental results from the study of material flow will be presented and compared with numerical calculation. Various interesting measurement techniques will also be discussed.

Keywords: Intense dynamic loading

1. INTRODUCTION

Explosively driven, cylindrically imploding FSTs can be configured to produce gas pressure at levels well above those achievable with planar high-explosive (HE) systems [1,2]. Potentially, such device can accelerate plates to velocities much higher than those possible with light gas guns, and thus can be very valuable for studying equations of state, material property, and impact phenomena in higher pressure regime. Our earlier attempts to accelerate thin plates with the FST have resulted in premature breakup due to severe radial velocity, density, and pressure gradients [3]. We have succeeded in mitigating some of these problems [4], and results from more recent work will be discussed below.

2. FAST SHOCK TUBE

A simple FST is illustrated in Fig. 1a. It is made up of a hollow outer HE cylinder and filled styrofoam core. The HE is single-point ignited at the left end with a plane wave lens. Due to the phased implosion, the inner HE wall converges radially and acts as a peristaltic pump to push foam to the right. The subsequent dynamics are readily understood via the physics of steady-state nozzle flow [5,6]. A Mach disk is generated in the foam core as the oblique shock intersects the reflection from the axis. The axial shock front continues to develop as the HE burn continues. In a properly designed system, the Mach disk is fully developed at the exit end and the flow of compressed foam behind is smooth with almost no radial gradients and very gradual axial gradients. The velocity of the shock front can exceed the HE detonation velocity, but generally a slightly under-driven situation is preferred to avoid predetonating the HE ahead.

In designing an optimized system, balance is achieved by adjusting the inner to outer diameter ratio of the HE, the length, the density of the foam, and the phase velocity between the detonation wave and the interface. Foam density variation is often a practical degree of freedom for fine adjustment. A 2D Eulerian hydrocode has been used to determine the parameters in Fig. 1a. In the calculation, the JWL equation of state is used for the explosive products with programmed burn [7]. Treating the lower-density CH foam as ideal gas with gamma of 5/3, appears to be in good agreement with experimental observation. A radiograph showing the detonation front, the reflected shock, and the Mach disk can be seen in Fig. 1b, along with a code simulation showing their agreement. In time, the Mach disk is fully developed and travels down in phase with the burn front. Test and calculation with time-lit arrangement results in an oblique detonation front but the characteristics of the axial shock remain unchanged. We have also found that the planar shock generated in the foam travels nearly perpendicularly to the center line even if the HE detonation is not per

*This work was supported by the US Department of Energy.

fectly symmetrical or if the foam density is not too uniform.

Other diagnostics, which often are more intrusive than x-ray radiography, have also been employed to characterize the axial shock in the various FST experiments. A Doppler-shift microwave interferometer [8] was used to measure shock velocity and symmetry by placing a number of micro-coaxial cables (0.35-mm-diameter) at the interface and inside the foam. A Xenon flasher assembly [9] placed at the end enabled us to measure the final shock planarity and velocity with a smear camera. Single-mode quartz fibers inserted inside the foam provided a means for tracking the temporal and spatial behaviors of the shock. Attempts to determine the shocked quartz temperature using time-resolved optical radiation measurement, and thus the impinging shock history by impedance matching, appears to be more complicated. Measurements with the above diagnostics have yielded much critical information on the performance of the FST. The 0.32-g/cc foam, which has reasonably fine porosity and uniformity, is shocked to almost 1.8 g/cc and vaporizes rapidly. The expanding gas from the end of the shock tube is observed by optical shadowgraph to be moving as fast as 30 km/s.

3. PLATE ACCELERATION

Under an applied pressure pulse, $P(t)$, a plate of density, ρ, and thickness, l, will experience an acceleration, $a(t)$, according to the relation $P(t) = \rho l a(t)$. The final plate velocity, v, is governed by the impulse equation $\int P dt = mv$, where m is mass per unit area. Two systems have been studied to accelerate 0.15-cm thick SS plates. The first system, fast shock tube without barrel (FSTN), is configured, as illustrated in Fig. 2a, by simply placing an SS plate at the end of the FST. The second system, fast shock tube with barrel (FSTB), which incorporates a steel barrel with a smaller inner diameter one half that of the HE/foam interface and a 0.32-cm stand off, is shown in Fig. 2b.

In the FSTN system the Mach disk grows to the full unshocked foam diameter and arrives at the plate simultaneously with the detonation front. The plate thus experiences an extremely flat impulse but suffers a very strong shock loading. A hydrocalculation result is shown in Fig. 3a and a radiograph of a 0.15-cm SS plate is shown in Fig. 3c. The comparison of the plate profile shows close agreement. The plate appears to stay together as it travels downstream into a witness plate. The radiograph indicates a plate velocity of only 6.2 km/s as compared to 7.4 km/s in the calculation. The discrepancy is attributable to the early pressure relief as the central portion of the plate is punched out of the periphery by the stronger Mach structure.

The severity in plate loading can be seen in Fig. 3c where calculation shows the initial loading rate on-axis to exceed 8 Mbar/μs before the stagnation reaches a peak of 0.8 Mbar. Off-axis loading profile is similar but with lower peak pressure consistent with gases escaping. The code uses material strength [10] but no fracture model is available. It is worth mentioning that when a more ductile but lower strength Ti(6,4) plate of the same areal density is accelerated, the plate balloons nearly to a full hemisphere before bursting. Experiments with plates of higher yield strength but lower ductility usually result in quick fragmentation. Attempts to accelerate thinner SS plates generally end in early breakthrough at the center and result in lower rather than higher velocity. The detail of why the SS plate responds more favorably in this particular loading environment is still being studied. We have, however, found that by doubling the length of the FST, the profile of the projectiles consistently appears flatter even though the plate remains fragmented and the velocity does not increase noticeably. It is clear that we need to understand more about the balance between the applied impulse and the dynamic material response.

The barrel in the FSTB system serves to confine the pressure behind the plate longer and thus increases the effective impulse. Calculations show that the plate velocity rises when the wall thickness increases from 0.2 to 1.5 cm, but the length becomes unimportant after a few centimeters. Expansion and cooling of gases into a standoff gap will result in a more gentle stagnation against the plate.

A plate drive calculation is shown in Fig. 4a. The forward concave feature is derived from earlier design experience to free the plate from the barrel wall and to prevent the unstable radial stretching. The desired configuration is facilitated by the early collapse of the inner barrel corner, which causes the gas to accelerate the periphery of the SS plate first. In the calculation, the shape of the plate remains stable in time and the plate velocity quickly reaches 10 km/s. In the calculation, the plate appears to be thinning, and apparently with less mass than the observation. This may explain why it is faster. Again, gas relief around the periphery is also a factor.

The calculated loading rate is apparently much smaller than in the FSTN system, as can be seen in Fig. 4c where it is reduced to about 1 Mbar/μs. However, the peak pressure is increased to 1.6 Mbar due to gas confinement. The structure in the pressure profile is an indication of complicated flow dynamics going on inside the stand-off channel. Many undesirable 2D problems are created. In some experiments, we have confirmed the calculated velocity and pressure profiles directly by VISAR [11] and Fabry-Perot interferometry measurement. However, the optical tracking time is limited by the opacity of expanding HE products. We have also found that the reflectivity of a highly shocked surface can be abruptly modified.

Experiments with larger barrel ID or with different plate materials all tend to end in early fragmentation. The only exception is a layered sapphire-Ti plate, which we have successfully accelerated to 11 km/s before fracturing, while the debris stays in a plane and travels downstream with very small divergence. It will be interesting to find out if a high sound speed buffer material can be effectively used to help mitigate the impact of shock loading. Several experiments were performed on a geometrically scaled-up system with 13.5 cm outer HE diameter, 2.5 cm inner barrel diameter, and 0.85 cm standoff. Under acceleration, a 4 mm thick SS plate is fragmented into big chunks at a velocity of 8.1 km/s. As expected, the uncertainties are primarily due to our inability to handle the mass flow properly inside the scaled-up channel.

4. Conclusions

We have successfully accelerated a thin SS plate to 9 km/s with a single phase detonated FST system. This success is made possible by making sure (a) that the Mach disk at the output end of the phased implosion is fully developed, (b) that the propellant flow is kept planar in as large an impacted plate area as possible, and (c) that the periphery of the plate is separated from the wall early. In principle, higher plate velocity can be achieved with higher phase detonation velocity device. In practice, we have learned that accelerating the plate under intense impulse is very challenging. We need to understand more about the details of high-pressure hydrodynamics and dynamic material response before significant progress is possible.

REFERENCES

1. G. H. McCall, "A Method for Producing Shockless Acceleration of Masses to Hypervelocity Using High Explosives," La Jolla Institute, LJI-TM-166, La Jolla, CA (May 1984).
2. R. D. Steel and T.-H. Tan, "Fast Shock Tube Assemblies," in *Shock Waves in Condensed Matter 1987*, Eds. S. C. Schmidt and N. C. Holmes (North-Holland, 1987), p. 661.
3. T.-H. Tan, J. N. Fritz, S. P. Marsh, R. G. McQueen, and R. D. Steel, "Characterization of Simple Explosively Driven Particle Accelerator, in *Shock Waves in Condensed Matter 1987*, Eds. S. C. Schmidt and N. C. Holmes (North-Holland, 1987), p. 665.
4. S. P. Marsh and T.-H. Tan, "Hypervelocity Plate Acceleration," *1991 APS Topical Conference on Shock Compression of Condensed Matter*, Williamsburg, VA (June 1991), to be published.
5. R. Menikoff, K. S. Lackner, N. L. Johnson, S. A. Colgate, J. M Hyman, and G. A. Miranda, "Shock Wave Driven by a Phased Implosion," *Phys. Fluids A* 3 (1), 201 (1990).
6. J. K. Meier and J. F. Kennedy, "An Introduction to the Fast Shock Tube," *1991 APS Topical Conference on Shock Compression of Condensed Matter*, Williamsburg, VA (June 1991), to be published
7. B. M. Dobratz and P. C. Crawford, LLNL Explosives Handbook, Properties of Chemical Explosives and Explosive Simulants, Report No. UCRL-52997
8. G. H. McCall, W. L. Bongianni, and G. A. Miranda, *Rev. Sci. Instrum.* 56 (8), 1612 (1985)

9. J. M. Walsh and R. H. Christian, *Phys. Rev.* **97**, 1544 (1955).
10. D. J. Steinberg, S. G. Cochran, and M. W. Guinan, "A Constitutive Model for Metals Applicable at High-Strain Rate," *J. Appl. Phys.* **51** (3), 1498 (1980).
11. L. M. Barker and R. E. Hollenbach, *J. Applied Phys.* **43**, 4669 (1972).

Fig. 1. (a) Simple FST configuration and (b) overlay of calculated and radiographic wave fronts in foam and HE.

Fig. 2. Configuration of plate accelerators. (a) FSTN, accelerator without barrel, (b) FSTW, accelerator with barrel.

Fig. 3. (a) Overlay of FSTN setup and dynamic calculation, (b) radiograph of SS plate at 4 μs apart, and (c) calculated pressure profile.

Fig. 4. Overlay of FSTW setup and dynamic calculation, (b) radiograph of SS plate at 4 μs apart, and (c) calculated pressure profile.

a

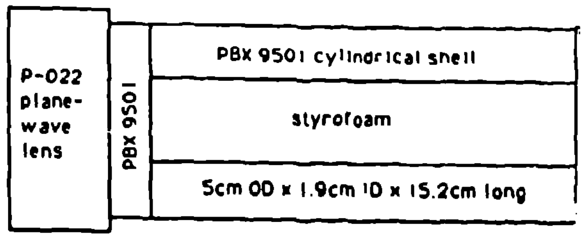

b

FIGURE 1

(a) Simple FST configuration and (b) overlay of calculated and radiographic wave fronts in foam and HE a

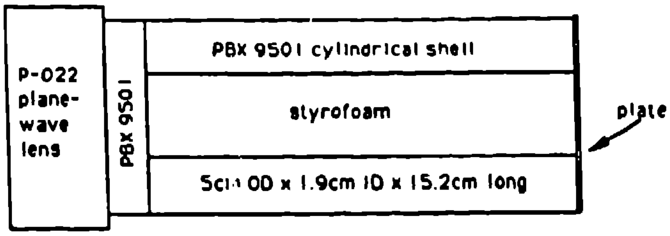

b

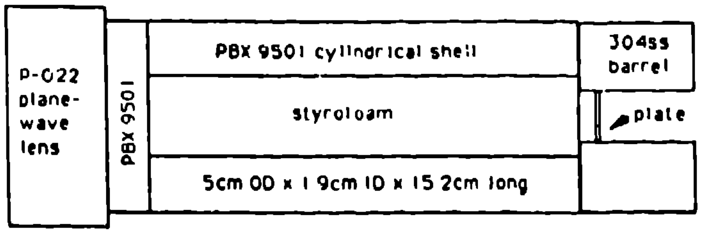

FIGURE 2

Configuration of plate accelerators. (a) FSTN, accelerator without barrel. (b) FSTW, accelerator with barrel.

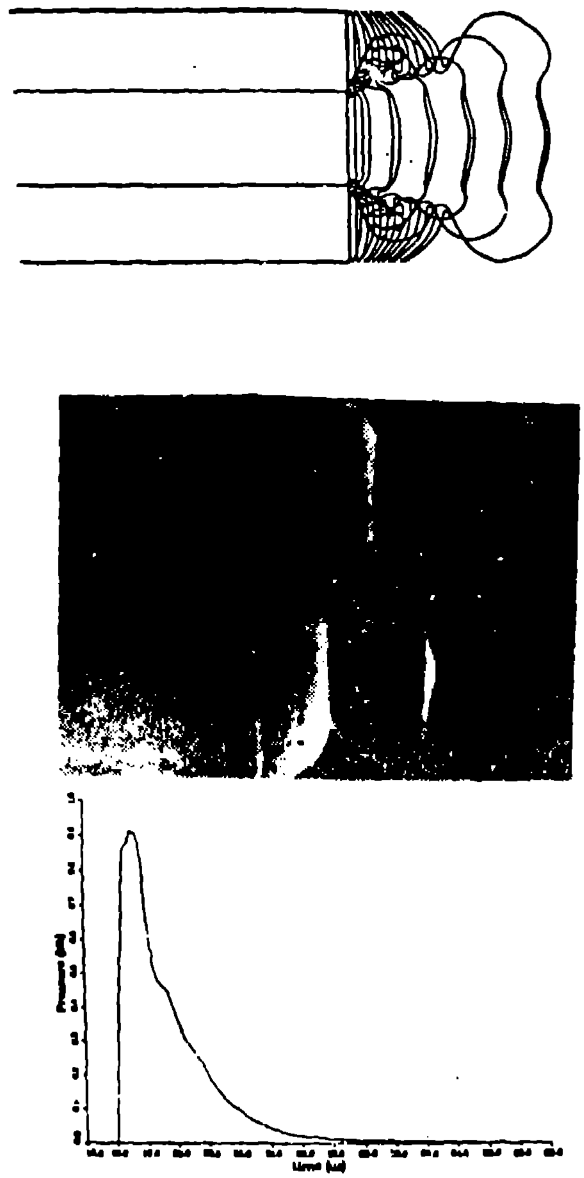

FIGURE 3
(a) Overlay of FSTN setup and dynamic calculation, (b) radiograph of SS plate at 4 μs apart, and (c) Calculated pressure profile.

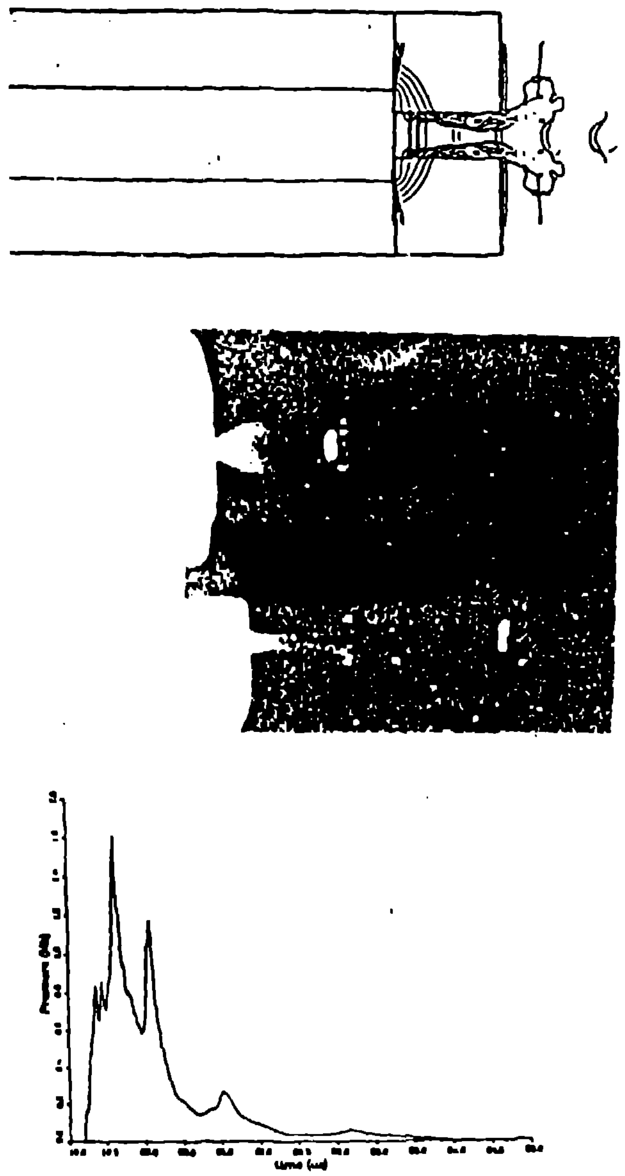

FIGURE 4
(a) Overlay of FSTW setup and dynamic calculation, (b) radiograph of SS plate at 4 μs apart, and (c) Calculated pressure profile.